Acta Cryst. (1995). D**51**, 682–694

TEM1 β-Lactamase Structure Solved by Molecular Replacement and Refined Structure of the S235A Mutant

BY E. FONZÉ,* P. CHARLIER* AND Y. TO'TH

Centre d'Ingénierie des Protéines, Unité de Cristallographie, Université de Liège, Institut de Physique, B5, B4000 Sart Tilman, Liège, Belgium

M. VERMEIRE

Unité de Cristallographie, Université de Liège, Institut de Physique, B5, B4000 Sart Tilman, Liège, Belgium

AND X. RAQUET, A. DUBUS AND J.-M. FRÈRE

Centre d'Ingénierie des Protéines and Laboratoire d'Enzymologie, Université de Liège, Institut de Chimie, B6, B4000 Sart Tilman, Liège, Belgium

(*Received* 20 *June* 1994; *accepted* 12 *December* 1994)

Abstract

β-Lactamases are bacterial enzymes which catalyse the hydrolysis of the β-lactam ring of penicillins, cephalosporins and related compounds, thus inactivating these antibiotics. The crystal structure of the TEM1 β-lactamase has been determined at 1.9 Å resolution by the molecular-replacement method, using the atomic coordinates of two homologous β-lactamase refined structures which show about 36% strict identity in their amino-acid sequences and 1.96 Å r.m.s. deviation between equivalent Cα atoms. The TEM1 enzyme crystallizes in space group $P2_12_12_1$ and there is one molecule per asymmetric unit. The structure was refined by simulated annealing to an R factor of 15.6% for 15 086 reflections with $I \geq 2\sigma(I)$ in the resolution range 5.0–1.9 Å. The final crystallographic structure contains 263 amino-acid residues, one sulfate anion in the catalytic cleft and 135 water molecules per asymmetric unit. The folding is very similar to that of the other known class A β-lactamases. It consists of two domains, the first is formed by a five-stranded β-sheet covered by three α-helices on one face and one α-helix on the other, the second domain contains mainly α-helices. The catalytic cleft is located at the interface between the two domains. We also report the crystallographic study of the TEM S235A mutant. This mutation of an active-site residue specifically decreases the acylation rate of cephalosporins. This TEM S235A mutant crystallizes under the same conditions as the wild-type protein and its structure was refined at 2.0 Å resolution with an R value of 17.6%. The major modification is the appearance of a water molecule near the mutated residue, which is incompatible with the OG 235 present in the wild-type enzyme, and causes very small perturbations in the interaction network in the active site.

* Authors to whom correspondence should be addressed.

Introduction

β-Lactamases are penicillin-destroying enzymes which were discovered even before the introduction of β-lactams as chemotherapeutic agents. New enzymes, which exhibit very diverse substrate specificities and sometimes very different primary structures, are continuously discovered and described.

The chemistry of their catalytic mechanisms divides the β-lactamases into two groups. The first includes zinc enzymes and are indexed as class B enzymes. All the other β-lactamases described so far fall into the second group and are active-site serine enzymes. According to their amino-acid sequences they are subdivided into three classes A, C and D, but they all follow a similar kinetic scheme, involving an acyl-enzyme intermediate ES* (Waley, 1992; Ledent, Raquet, Joris, van Beeumen & Frère, 1993),

$$E + S \underset{k_{-1}}{\overset{k_{+1}}{\rightleftarrows}} ES \xrightarrow{k_2} ES^* \xrightarrow[H_2O]{k_3} E + P.$$

Class A and C β-lactamases also share the same general secondary-structure pattern as shown by superimposing the known three-dimensional structures determined by X-ray crystallography: *Staphylococcus aureus* PC1 (Herzberg, 1991), *Bacillus licheniformis* 749/C (Moews, Knox, Dideberg, Charlier & Frère, 1990), *Streptomyces albus G* (Dideberg *et al.*, 1987) and *Escherichia coli* TEM (Strynadka *et al.*, 1992; Jelsch, Mourey, Masson & Samama, 1993) enzymes for the 29–30 kDa class A β-lactamases, *Citrobacter freundii* (Oefner *et al.*, 1990) and *Enterobacter cloacae* P99 (Lobkovsky *et al.*, 1993) enzymes for the 39 kDa class C β-lactamases. It is also interesting to mention structural similarities with the *Streptomyces* R61 DD-carboxypeptidase-transpeptidase (Kelly *et al.*, 1986), which corroborate the hypothesis of a common gene ancestor for all active-site serine penicillin-recognizing

ISSN 0907-4449

enzymes. Nevertheless, the observed divergence between the different β-lactamase classes and/or the different penicillin-binding protein (PBP) groups, is too high to derive accurate three-dimensional models for a class D β-lactamase or a PBP from the presently known structures (Joris *et al.*, 1988).

The class A β-lactamases are synthesized either by Gram-negative or Gram-positive bacteria, and the corresponding genes are found both on plasmids and on the chromosome. Their catalytic properties are extremely different, reflecting a wide diversity in their primary structures, in contrast to the other β-lactamase classes.

Following the massive clinical utilization of β-lactamase-stable compounds, such as the oxyimino-β-lactam cefotaxime, ceftazidime and aztreonam, against the most widespread pathogenic strains, an increasing number of resistant isolates have emerged within a few years all over the world. The resistance could be attributed to a combination of different phenomena amongst which the occurence of mutants in the SHV and TEM class A enzymes exhibiting hydrolytic properties *versus* the so-called β-lactamase-stable antibiotics (see for instance, Jacoby & Medeiros, 1991). These extended-spectrum β-lactamases show mutations at strategic positions in the active site or in its vicinity, such as E104K near the SDN motif, R164S/H upstream helix *h*7, A237T/G, G238S and E240K on the *b*3 strand. Generally the increase of activity against oxyimino compounds is accompanied by a decrease of activity *versus* good substrates such as benzylpenicillin and cephaloridin (Healey, Labgold & Richards, 1989; Sowek *et al.*, 1991). Usually these enzymes remain sensitive to the inactivators clavulanate and sulbactam.

We report here the structure of the TEM1 β-lactamase as determined by molecular replacement, the first β-lactamase structure entirely solved by this method, except those of two β-lactamase mutants determined from their corresponding native enzyme: the *Bacillus licheniformis* 749/C E166A mutant (Knox, Moews, Escobar & Fink, 1993) and the *Staphylococcus aureus* PC1 D179N mutant (Herzberg, 1991), whose PDB entry codes are 1MBL and 1BLP, respectively (Bernstein *et al.*, 1977). The use of the molecular-replacement methodology in previous structural studies of TEM1 β-lactamase, carried out by Strynadka *et al.* (1992) and Jelsch *et al.* (1993) has failed. One explanation could be too low a similarity with the probe structure, namely the *Staphylococcus aureus* PC1 β-lactamase (1BLM and 3BLM entry codes). To construct a search model of TEM1, we could rely on crystallographic structures of two more similar class A β-lactamases, those of *Bacillus licheniformis* 749/C, named Bl (PDB entry code 4BLM), and of *Streptomyces albus* G, or SaG, refined at 1.7 Å resolution (personal unpublished results). So, this was a good opportunity to test the limitation of molecular replacement in the case of a class of enzymes that exhibits a wide variety of amino-acid sequences. On the other hand, the enzymatic properties of the TEM enzyme have been widely studied. Kinetic information about both naturally occuring and site-directed mutants is available. We plan to analyse their structures in order to contribute to an improved insight into the catalytic mechanism and the substrate specificity of the class A β-lactamases. Here we describe the structure of the S235A TEM mutant, obtained by site-directed mutagenesis (Dubus, Wilkin, Raquet, Normark & Frère, 1995) and determined from the atomic coordinates of the native enzyme. Residue 235 is part of the highly conserved KS(T)G motif, which forms a wall of the catalytic cleft. This mutation has little impact on the penicillinase activity, but decreases the cephalosporinase activity in a much more significant manner (Dubus *et al.*, 1995).

The TEM1 structure is also compared with the three other known β-lactamase structures: Bl, SaG and Sa for the *Staphylococcus aureus* PC1 enzyme.

Materials and methods

Purification and crystallization

The TEM enzymes were produced and purified from *Escherichia coli* harbouring either the ptac11 (wild type) or pAD27 (S235A mutant) plasmid (Amman, Brosius & Ptashne, 1983; Dubus *et al.*, 1995). Purification was achieved in two steps by successive chromatographies on a Q-Sepharose Fast Flow column at pH 7.5 and 6.5, respectively.

TEM1 wild-type crystals were grown by the vapour-diffusion method using a wild-type protein concentration of 20 mg ml^{-1} in various buffer and pH conditions (from pH 6.75 to 7.50) with ammonium sulfate as precipitating agent. The best crystals were prisms of 0.9 × 0.25 × 0.25 mm and grew over a period of one to four weeks at 292 K in 0.1 *M* imidazole pH 7.0, containing 10 m*M* NaN_3 and ammonium sulfate at 43–48% saturation.

The crystallization of the TEM S235A mutant was initiated under the same conditions by the microseeding technique, small crystals of the TEM1 wild-type enzyme being used as microseeds. Microcrystals obtained from this cross-seeding were used to repeat experiments to dilute out the effect of heterogenous seeds.

Data collection and processing

The TEM1 crystals are orthorhombic with unit-cell parameters $a = 41.8$, $b = 62.7$ and $c = 89.8$ Å, space group $P2_12_12_1$. There is one molecule per asymmetric unit which gives a crystal volume per unit molecular mass of 2.03 Å^3 Da^{-1} and a solvent content of 39.5% by volume.

X-ray diffraction data were collected at 293 K with a Siemens X100 area detector. The X-ray source was graphite-monochromated Cu $K\alpha$ radiation produced by a Rigaku RU-200 rotating-anode generator operating

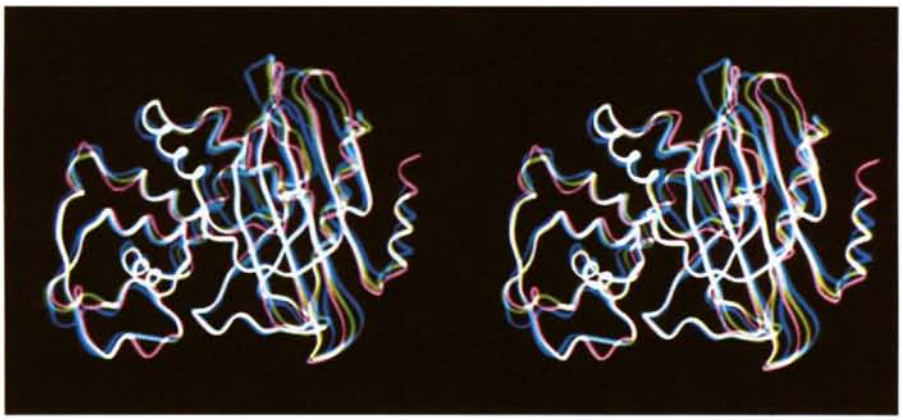

Fig. 1. Superposition of the three β-lactamase structures represented as ribbons: *Bacillus licheniformis* (green), *Streptomyces albus* G (magenta) and *Staphylococcus aureus* (blue). Prepared with *O* (Jones, Zou, Cowan & Kjelgaard, 1991).

at 40 kV and 120 mA. The detector was positioned at 150 mm from the crystal. Five complementary sets were collected on the same crystal. It was first mounted with the long axis parallel to the incident beam, two sets at high resolution ($2\theta = 30°$) with two different positions of φ-circle ($\varphi = 0°$ and 45°) and one set at low resolution ($2\theta = 15°$) were collected. The same crystal was then moved inside the capillary so that the long axis was perpendicular to the incident beam: two sets ($2\theta = 15°$ and 30°, $\varphi = 0°$) were again recorded. For each orientation of the crystal, 500 frames were collected, covering on the whole a 100° rotation of the ω-circle. In a single frame, reflections resulting from a 0.2° oscillation of the crystal were recorded in 60 s.

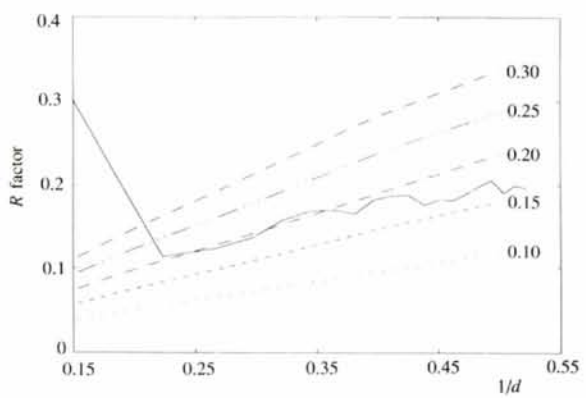

Fig. 2. Luzzati (1952) plot for the refined TEM1 structure: *R* factor *versus* the inverse of the resolution, with the theoretical curves corresponding to mean coordinate errors of 0.10 to 0.30 Å.

Crystal orientation and integrated intensities were calculated with the *XENGEN* Version 2.0 software (Howard *et al.*, 1987). After scaling, 67 369 recorded reflections were obtained with a weighted-squared merging R_{sym} on intensity of 4.22%. These merged data yielded 17 252 unique reflections (Table 1).

For the S235A TEM mutant, cell parameters were $a = 41.9$, $b = 63.2$ and $c = 88.7$ Å and the other crystal properties were the same as those of the wild-type enzyme. The X-ray diffraction data were collected and processed as described above and yielded 48 113 scaled reflections with an R_{sym} of 3.5%. After merging 17 496 unique observations were obtained (Table 1).

Structure determination and refinement

The crystal structure of the TEM1 β-lactamase was determined by the molecular-replacement technique. The *MERLOT* (Fitzgerald, 1988) package of programs, which

Fig. 3. Schematic (stereo) drawing of TEM1: β-strands are drawn as red arrows, helices as spirals, in green and in magenta for the α-helices and 3_{10}-helices, respectively. The active serine S70 is represented in CPK mode. Prepared with *O* (Jones *et al.*, 1991).

includes the fast rotation function of Crowther (1972), the rotation function of Lattman & Love (1970) and, a translation function of Crowther & Blow (1967), was used throughout. The starting model for the rotational and translational parameter investigations was based on the two most similar class A β-lactamase refined structures, those of *Bacillus licheniformis* (Bl) and *Streptomyces albus* G (SaG) which exhibit 35% of identical residues. The TEM1 model was constructed using the *FRODO* program package (Jones, 1985) on an Evans & Sutherland PS330. It corresponds to the Bl structure where the side chains have been replaced by the corresponding ones in the TEM1 sequence except in the 84–90 loop where the SaG structure was used (Fig. 1). Another TEM1 model, called partial, was also tested, and corresponds to the polyalanine chain of well conserved regions between the three class A β-lactamase structures (Bl, SaG and Sa) in addition to the strictly conserved side chains between Bl and TEM1.

The orientation of the TEM1 model in the unit cell $P2_12_12_1$ was searched with both complete and partial models at various resolution ranges: 20–4, 10–4, 8–3 and 8–2.5 Å. The highest peaks of the rotation functions varied around Eulerian angles $\alpha = 120$, $\beta = 63$, $\gamma = 300°$. This orientation was refined using the *X-PLOR* PC-refinement (Brünger, 1992), and a significant correlation

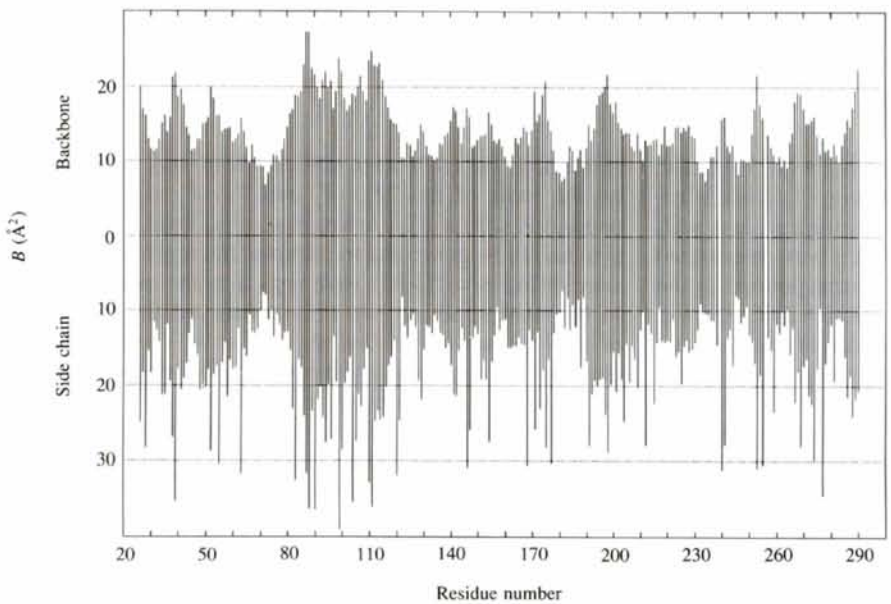

Fig. 4. Temperature-factor distribution along the amino-acid sequence of TEM1 for the backbone (upper) and side-chain (lower) atoms, respectively.

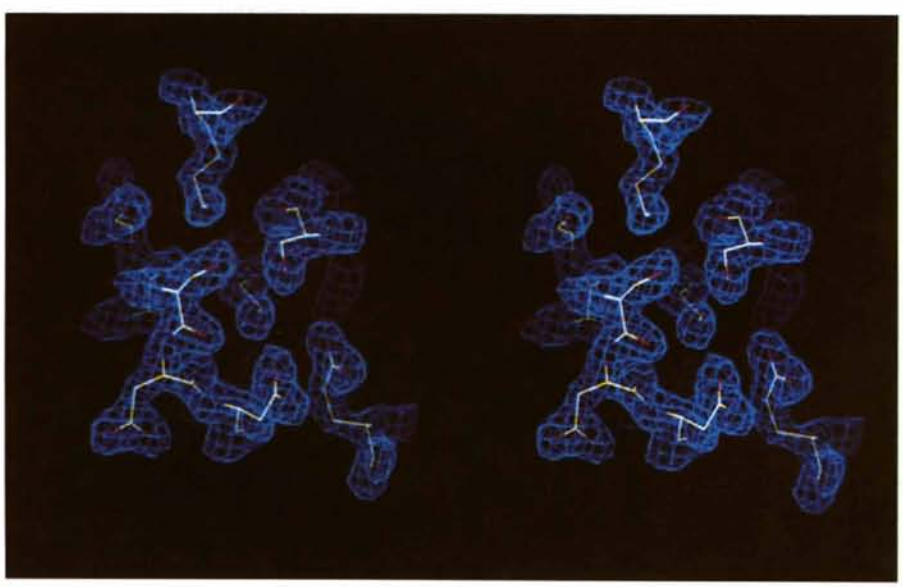

Fig. 5. Stereoview of the active serine and the SDN loop in the $2F_o - F_c$ electron-density map contoured to 1.1σ above the mean.

Table 1. *Summary of observations by resolution shell for the TEM1 wild-type enzyme and the TEM S235A mutant enzyme*

I represents the average intensity for all scaled observations of a reflection.

Shell lower limit (Å)	Average resolution (Å)	Average $I/\sigma(I)$	No. of Bragg reflections Possible	Collected	Completeness (%)
(*a*) TEM1 wild-type enzyme					
3.34	4.49	127.2	3699	3636	98.3
2.65	2.94	51.3	3503	3328	95.0
2.32	2.47	24.5	3477	3053	87.8
2.10	2.20	16.6	3449	2894	83.9
1.95	2.03	9.9	3460	2731	78.9
1.84	1.91	5.2	3397	1610	47.4
Totals	2.58	45.9	20985	17252	82.2
(*b*) TEM S235A mutant enzyme					
3.20	4.30	96.3	4243	4294	98.8
2.54	2.81	32.5	4047	3779	93.4
2.22	2.36	16.5	4000	3227	80.7
2.01	2.11	10.2	3984	2852	71.6
1.87	1.94	5.1	3978	2284	57.4
1.76	1.83	2.5	3922	1160	29.6
Totals	2.55	35.6	24174	17496	72.4

between F_{obs} and F_{calc} was only observed with the partial model. This can be explained by the sum of errors introduced in the complete model by modelling of less well conserved regions. The final orientation was determined between 8 and 2.5 Å resolution and corresponded to the Eulerian angles $\alpha = 121.00$, $\beta = 63.19$, $\gamma = 299.80°$.

To position the oriented model in the crystal, several tests were performed with the complete and partial models, at different resolution ranges. Only the complete model at a resolution of 3 Å or more yielded a clear translation solution $x = 0.380$, $y = 0.035$, $z = 0.135$, compatible with the three Harker sections $u = 1/2$, $v = 1/2$, $w = 1/2$. The corresponding molecular packing was quite acceptable. It is worth noting here that the TEM1 crystal packing is much denser than those of the other class A β-lactamases because of the smaller unit-cell dimensions. To improve the molecular-replacement solution, several rigid-body refinements (*X-PLOR*) were applied to the partial model at 3 Å resolution and yielded an *R* factor of about 48% with a correlation of 39.9% between the observed and calculated structure factors. This polyalanine positioned model was then used to compute first maps ($2F_o - F_c$ and $F_o - F_c$) between 20.0 and 3.0 Å resolution, which showed the well conserved secondary elements and the largest side chains.

It is interesting to note that at this stage, we received the *AMoRe* molecular-replacement package (Navaza, 1994) and tested its efficiency. At all resolution ranges, with both complete or partial models, the molecular-replacement solution (rotation, translation and rigid-body refinement) was obtained in a very short time.

The refinement procedure was performed by simulated annealing with the *X-PLOR* program package. The several alternating cycles of refinement (positions, temperature factors) and model refitting (*FRODO*, PS330) are summarized in Table 2. The final *R* value is 15.6% for 15 086 reflections with $I \geq 2\sigma(I)$ between 5.0 and 1.9 Å resolution. At each step, the structure was constructed on the basis of the $2F_o - F_c$ and $F_o - F_c$ maps, always computed with a 20 Å lower resolution limit. Omit maps also had to be generated to interpret the regions that were very different in TEM1 with regard to the initial model. In the final structure, we only conserved the first layer of solvent molecules that showed a very well defined electron density and a temperature factor less than or equal to 60 Å^2. Comparison between the *R* factor in terms of resolution and theoretical curves with various mean coordinate errors (Luzzati, 1952) shows that the upper limit of the mean positional atomic error is about 0.20 Å (Fig. 2).

Results and discussion

Overall structure

The refined structure contains 263 amino-acid residues and the polypeptide chain exhibits the typical folding observed in the known class A β-lactamase structures (Fig. 3). It consists of two globular domains: one is formed by a five-stranded antiparallel β-sheet (*b*1 to *b*5) covered by the two terminal α-helices (*h*1, *h*11) and a short 3_{10}-helix (*h*10) on one face and one α-helix (*h*8) on the other face. The second domain contains a big central α-helix (*h*2) surrounded by four α-helices (*h*4, *h*5, *h*6 and *h*9) and three 3_{10}-helices (*h*3*a*, *h*3*b* and *h*7).

The electron density overall is well defined,with the exception of some solvent-exposed side chains (Q39, Q88, Q90, Q99, E104, K111, K146, K215 and E274) and which correspond to the highest temperature-factor values (Fig. 4). A classical $2F_o - F_c$ map computed at the last refinement cycle shows the electron density around the active serine S70 (Fig. 5). The stereochemistry is good with r.m.s. deviations of 0.013 Å for bond lengths, 2.8° for bond angles, 24.1° for fixed dihedral angles and 1.2° for improper dihedral angles. The distribution of

Table 2. *Refinement parameters and process of the R factor as a function of refinement steps using the X-PLOR molecular dynamics program*

WA is computed in the check stage and represents the ideal weight between crystallographic and empirical energies. Only reflections such as $I \geq 2\sigma(I)$ are used.

Step	No. of residues No. of atoms (no H) No. of solvent molecules	Resolution range (Å)	No. of reflections	Check stage	Preparation stage	Simulated annealing	*B*-factor refinement
1	256 AA 1610 atoms	6.0–2.5	7439	WA = 92221 *R* = 49.9%	*R* = 36.3%	*R* = 30.9%	—
2	258 AA 1943 atoms	6.0–2.5	7439	WA = 112150 *R* = 44.2%	*R* = 30.1%	*R* = 26.2%	—
3	255 AA 1902 atoms	6.0–2.5	7439	WA = 119140 *R* = 44.7%	*R* = 29.6%	*R* = 24.5%	—
4	260 AA 2001 atoms	5.0–2.0	13053	WA = 120660 *R* = 43.5%	*R* = 26.8%	*R* = 24.2%	*R* = 21.3%
5	263 AA 2109 atoms 1 SO_4, 77 HOH	5.0–2.0	13053	WA = 134390 *R* = 35.3%	*R* = 19.2%	*R* = 18.6%	*R* = 17.4%
6	263 AA 2193 atoms 3 SO_4, 151 HOH	5.0–1.9	15086	WA = 142920 *R* = 33.6%	*R* = 17.8%	*R* = 16.9%	*R* = 16.0%
7	263 AA 2167 atoms 1 SO_4, 135 HOH	5.0–1.9	15086	WA = 150140 *R* = 32.9%	*R* = 16.2%	*R* = 16.2%	*R* = 15.6%

the φ,ψ torsion angles that define the polypeptide backbone (Fig. 6) reveals specific conformations for Met69 ($\varphi = 54.9°$ and $\psi = -144.8°$) and Leu220 ($\varphi = -104.7°$ and $\psi = -121.5°$), as observed in all class A structures. Interestingly, these peculiar positions are situated at the junction between the two domains.

The protein is solvated by one sulfate anion in the catalytic cleft and 135 ordered water molecules mainly located in the first coordination shell, directly hydrogen bonded to protein atoms. Their mean temperature-factor value is 36.5 Å^2. The lowest *B*-factor values correspond either to outer water molecules involved in intermolecular water bridges in the crystal packing, or to inner water molecules located either in the active site such as WAT292 and WAT298 (Table 6), or located between secondary-structure elements (Table 3).

The three-dimensional structure of TEM1 is stabilized by a series of interactions: one cystine disulfide bridge

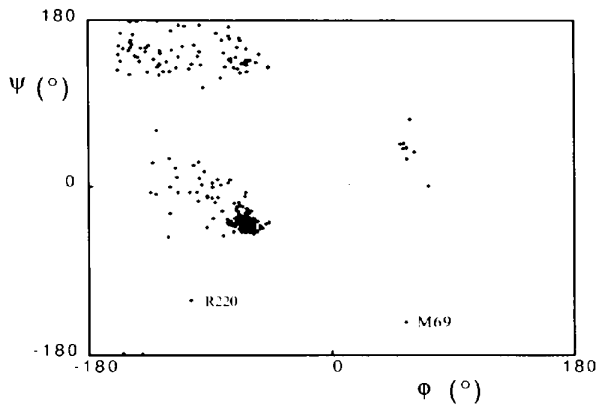

Fig. 6. Ramachandran plot for all residues except glycines (Ramachandran, Ramakrishnan & Sasisekharan, 1963).

Table 3. *Internal water molecules located between secondary-structure elements*

Water molecule identification	*B* factor (Å^2)	Amino-acid identification	Distance (Å)
WAT301	13.9	M68 NH	3.05
		M69 NH	2.75
		L169 O	2.89
WAT302	10.5	L169 O	2.62
		A172 NH NH	2.80
		WAT309 O	2.79
WAT310	16.0	I173 O	2.95
		D176 O	2.72
		WAT309 O	2.64
WAT311	25.0	R164 NH1	3.19
		I173 NH	2.95
		D176 OD1	2.80
		WAT309 O	2.84
WAT337	13.2	D214 O	2.74
		A217 NH	2.87
		WAT238 O	2.63
WAT354	10.1	A217 O	2.83
		L221 NH	2.81
		R222 NH	2.86
		D233 OD1	2.87
WAT397	19.3	K215 O	2.63
		G218 NH	2.89
WAT361	19.6	E48 OE1	3.17
		R259 NH2	3.11
		L286 O	2.89
		W289 O	3.10
		WAT418 O	2.91
WAT307	20.1	S242 O	2.73
		S268 NH	2.86
WAT387	28.0	L193 O	2.77
		G196 O	2.84
		L199 NH	2.91
		R204 NE	3.35

(Cys77–Cys123) which contributes to fix the central *h*2 α-helix within the α-domain, and a dozen of salt bridges listed in Table 4. Among these interactions, only the salt bridge involving R164 and D179 is conserved in all class A β-lactamase structures, ensuring the stability of helix *h*7 that defines the bottom of the active site

(Herzberg, Kapadia, Blanco, Smith & Coulson, 1991; Sowek *et al.*, 1991). Sequence alignments show that both residues are very well conserved in all class A β-lactamases (Ambler *et al.*, 1991; Nordmann & Naas, 1994) with the interesting exception of some TEM variants (Jacoby & Medeiros, 1991). These alignments also reveal that only a few class A β-lactamases (*Klebsiella pneumoniae*, PIT-2; *Pseudomonas aeruginosa*, PSE-4; *Rhodomonas capsulata* and *Streptomyces cacaoi*, blaU) have cysteine residues in equivalent positions (Ffaud 123). According to the mutagenesis experiment carried out on C77 (Schulz, Dalbadie–McFarland, Neitzel & Richards, 1987), it thus appears that this covalent link is not essential in the protein folding and in enzymatic activity.

Active-site structure

The catalytic cleft (Fig. 7), located at the interface between the two domains of the protein, is limited by the *b*3 strand, in particular by the K234-S235-G236 motif, the S130-D131-N132 loop, and the *h*7 helix

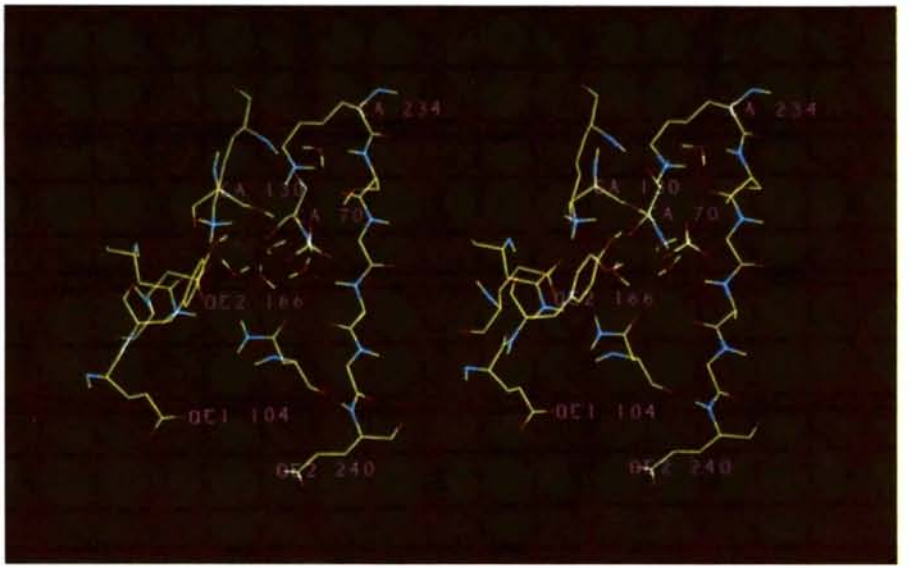

Fig. 7. Stereoview of the TEM1 catalytic cleft.

```
          ******h1******   ***b1***      **b2*            ******h2******              h3a
TEM1    HPETLVKVKDAEDQLGARVGYIELDLNSGKILESFRPEERFPMMSTFKVLLCGAVLSRVDAGQEQLGRRIHYSQNDL--VEYSP
B1      -----DDFAKLEEQFDAKLGIFALDT-GTNRTVAYRPDERFAFASTIKALTVGVLLQQKS--IEDLNQRITYTRDDL--VNYNP
SaG     -SDAERRLAGLERASGARLGVYAYDT-GSGRTVAYRADELFPMCSVFKTLSSAAVLRDLDRNGEFLSRRILYTQDDVEQADGAP
Sa      -----KELNDLEKKYNAHIGVYALDTKSGKE-VKFNSDKRFAYASTSKAINSAILLEQVP--YNKLNKKVHINKDDI--VAYSP
           30         40         50         60         70         80         90         100

 **h3b*       ****h4****    *****h5****  ****h6****              *h7             ******h8*****
VTEK--HLTDGMTVRELCSAAITMSDNTAANLLLTTIGGPKELTAFLHNMGDHVTRLDRWEPELNEAIPNDERDTTMPAAMATTLRKLLTGE
ITEK--HVDTGMTLKELADASLRYSDNAAQNLILKQIGGPESLKKELRKIGDEVTNPERFEPELNEVNPGETQDTSTARALVTSLRAFALED
ETGKPQNLANGMTVEELCEVSITASDNCAANLMLRELGGPAAVTRFVRSLGDRVTRLDRWEPELNSAEPGRVTDTTSPRAITRTYGRLVLGD
ILEK--YVGKDITLKALIEASMTYSDNTANNKIIKEIGGIKKVKQRLKELGDKVTNPVRYEIELNYYSPKSKKDTSTPAAFGKTLNKLIANG
110          120        130        140        150        160        170        180        190

   *****h9*****          *h10      ***b3***       ***b4***       ***b5***      *******h11*******
LLTLASRQQLIDWMEADKVAGPLLRSALPAGWFIADKSGAG-ERGSRGIIAALGPDGK-PSRIVVIYTTGSQATMDERNRQIAEIGASLIKHW-
KLPSEKRELLIDWMKRNTTGDALIRAGVPDGWEVADKTGAA-SYGTRNDIAIIWPPKG-DPVVLAVLSSRDKKDAKYDDKLIAEATKVVMKALN
ALNPRDRRLLTSWLLANTTSGDRFRAGLPDDWTLGDKTGAA-RYGTNNDAGVTWPPGR-APIVLTVLTAKTEQDAARDDGLVADAARVLAETLG
KLSKENKKFLLDLMLNNKSGDTLIKDGVPKDYKVADKSGQAITYASRNDVAFVYPKGQSEPIVLVIFTNKDNKSDKPNDKLISETAKSVMKEF-
200        210        220        230        240        250        260        270        280        290
```

Fig. 8. Alignment of the amino-acid sequences of the four class A β-lactamases determined from X-ray structure superposition: TEM1 from *E. coli*, Bl from *Bacillus licheniformis*, SaG from *Streptomyces albus G*, and Sa from *Staphylococcus aureus*. The secondary structures of TEM1, defined according to the Kabsch & Sander (1983) algorithm are shown above the sequences.

Table 4. *Salt bridges in the TEM1 structure*

Amino-acid identification	Amino-acid identification	Distance (Å)
K32 NZ	D35 OD1	2.96
K34 NZ	D38 OD2	3.02
R43 NH1	E64 OE2	2.98
R61 NE	E37 OE2	2.72
NH2	OE1	3.02
NH1	E64 OE1	2.80
R83 NH1	E89 OE1	3.16
R93 NE	E89 OE2	2.84
NH2	OE1	2.90
R161 NE	D163 OD1	2.94
NH2	OD2	2.75
R164 NH1	D179 OD1	2.76
NH2	E171 OE2	2.70
R178 NE	D176 OD1	2.76
NE	OD2	3.09
NH2	OD1	2.77
R222 NE	D233 OD1	3.12
NH2	OD2	2.99
R259 NH2	E48 OE1	2.99

Table 5. *List of interactions made by the conserved residue side chains in the catalytic cleft*

Amino-acid identification	Amino-acid identification	Distance observed (Å) TEM1	S235A
S70 OG	K73 NZ	2.79	2.94
	S130 OG	3.11	2.93
K73 NZ	S130 O	3.01	3.01
	N132 OD1	2.79	2.80
	E166 OE1	3.44	3.31
S130 OG	K234 NZ	2.83	2.99
N132 OD1	E166 OE1	3.21	3.13
	E166 OE2	3.27	3.34
N132 ND2	E104 O	2.97	2.93
E166 OE2	N170 ND2	2.94	2.88
N170 ND2	P167 O	3.28	3.29
K234 NZ	S235 O	2.81	2.93

that contains two amino-acid residues pointing into the site, E166 and N170. The active site also contains the nucleophilic serine residue S70 on the *h*2 α-helix and, three residues downstream, lysine K73. All these amino-acid residues are very well or strictly conserved among all class A β-lactamases, and many of them are also found in the class C and class D β-lactamases and in the penicillin-binding proteins (Joris *et al.*, 1991). Multiple site-directed mutagenesis experiments have been performed on these residues and have led to a better understanding and caracterization of their role in the catalytic process (Ellerby, Escobar, Fink, Mitchinson & Wells, 1990; Gibson, Christensen & Waley, 1990; Jacob, Joris, Lepage, Dusart & Frère, 1990; Brannigan, *et al.*, 1991; Juteau, Billings, Knox & Levesque, 1992; Knox *et al.*, 1993; reviewed in Matagne & Frère, 1995). Located at strategic positions in the active site, these amino-acid residues are involved in a structurally conserved dense hydrogen-bonding network (Table 5). Some solvent molecules, listed in Table 6, participate in that interaction scheme. The two water molecules, WAT292 and WAT298, are observed in the four class A β-lactamase structures and the first one has an identical position in all enzymes, underlining its crucial functional interest (Lamotte-Brasseur *et al.*, 1991).

Near the catalytic cleft, residues E104–Y105 lie in front of the SDN loop, and A237–E240 at the end of the *b*3 strand; as in SaG and Bl enzymes there is no residue in position 239. These amino acids are involved in substrate recognition by side-chain interactions and thus participate in determining the enzymatic profile or substrate specificity (Lenfant, Labia & Masson, 1990; Sowek *et al.*, 1991; Huletsky, Knox & Levesque, 1993).

Comparison with the other known class A β-lactamase structures

According to the sequence alignment generated by the superposition of the four class A β-lactamase refined structures (Fig. 8), the percentage of identical residue between the primary structures and the r.m.s. deviations between corresponding Cα atoms have been determined (Fig. 9). To compute these r.m.s. values, the 250 structurally equivalent CA atoms common to all four enzymes have been used; the following residues: 26–30, 52–57,

		Residue identity (%)			
		TEM1	**Bl**	**SaG**	**Sa**
	TEM1		35	37	32
r.m.s.	**Bl**	1.97		43	42
(Å)	**SaG**	1.94	1.05		28
	Sa	2.42	1.37	1.95	

Fig. 9. Lower part, r.m.s. deviations between the 250 equivalent Cα atoms of the four class A β-lactamase refined structures. Upper part, percentages of identical residue between the corresponding amino-acid sequences.

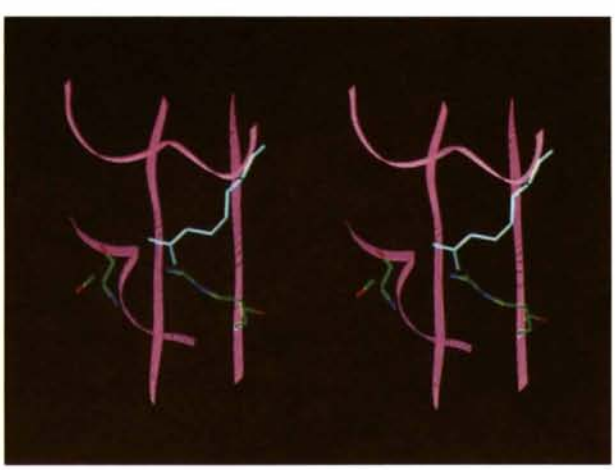

Fig. 10. Structural comparison of the orientation of the R244 side chain in TEM1 and R220 in SaG (in grey) relative to the active serine S70 of TEM1. The Cα trace is represented as a ribbon.

Table 6. *Solvent molecules in the TEM1 β-lactamase active site, associated temperature factors B and distances between the O atoms of the water molecules, the SO_4 ion and the amino-acid residues, and a comparison with the solvent molecules in the other β-lactamase structures*

Solvent molecule	*B* factor (Å²)	Amino-acid identification	Distance (Å)	Equivalent molecule in Bl	SaG	Sa
SUL291 O2	43.7	G237 NH	2.98	WAT692	HOH 1	HOH 64
		R244 NH2	2.76			HOH 71
SUL291 O4	46.7	S130 OG	2.83			HOH 111
		S235 O	2.85			
WAT292	16.2	S70 OG	2.84	WAT712	HOH 43	HOH 81
		S70 NH	3.06			
		E166 OE1	2.66			
		N170 OD1	2.73			
WAT293	39.3	S130 O	3.17	SUL600	HOH 72	HOH 42
		N132 OD1	3.17			
		SUL291 O1	3.02			
WAT294	34.1	SUL291 O3	2.71	WAT931	—	HOH 103
		Y105 OH 2.97				
WAT295	25.7	S70 OG	2.73	WAT672	HOH 73	HOH 22
		S70 NH	3.51			
		G237 NH	2.76			
		SUL291 O1	2.75			
WAT297	26.9	V216 O	2.73	WAT673	—	HOH 54
		R244 NH2	3.06			
		SUL291 O3	2.82			
WAT298	23.9	D214 OD2	2.75	WAT634	HOH 37	HOH 34
		K234 NZ	2.71			
		S235 OG	2.73			
		S235 NH	2.83			

86–87, 102a–102b–111a–111b of SaG, and 239–256 of Sa have been omitted.

When compared to the three other β-lactamases, TEM1 appears to be the most different structure with a mean r.m.s. of 2.11 Å compared with 1.47, 1.65 and 1.91 Å for Bl, SaG and Sa, respectively. However, the main variations in the general folding do not affect the amino-acid residues directly involved in the active site: (1) the N- and C-terminal residues adopt different conformations in the four enzymes; (2) the 51–55 loop is similarly folded in the TEM1 and Sa structures but is different in SaG and Bl where one amino acid has been deleted; (3) the 84–89 structural region is certainly the most variable in the class A β-lactamases in correlation with the observed amino-acid sequence differences; (4) the 254–257 loop folds differently in TEM1 compared to the three other structures, certainly because of the presence of a proline in position 257 instead of a proline 258; and (5) surprisingly, the loop (*b*5, *h*11) which is very well conserved in the Bl, SaG and Sa β-lactamases, adopts a very different conformation in TEM1. This may partly explain the more compact crystal structure. This perturbation is certainly due to the presence of a glycine in position 267 which permits special torsion angles for the TEM1 polypeptide chain (φ = 102, ψ = −19°) and the presence of a bulky residue (Met) in replacement of Ala or Asp in the other β-lactamases.

With respect to the two previously reported TEM1 structures, our results can only be compared with those of Jelsch *et al.* (1993); Strynadka *et al.* (1992) have not yet published details of their work. The TEM1 structure described by Jelsch has been refined at a higher resolution (1.8 Å) and contains more solvent molecules. Roughly, the geometric parameters such as deviations from ideal values and coordinate errors are close to ours. Their structure analysis reveals the same features: principal interactions, differences with the other class A β-lactamase structures, active-site topology, (φ,ψ) and temperature-factor distributions. Meanwhile, their *B* factors are lower than ours, certainly because they have worked at a higher resolution with more complete data and they have refined the atomic occupancy factors. Their catalytic cleft is also solvated by one sulfate anion and by water molecules WAT297, WAT323, WAT402 and WAT309 equivalent to WAT292, WAT295, WAT297 and WAT298 described here, respectively (Table 6). The only observed difference is that the SO_4 anion (SUL291) is positioned further within the active-site pocket and closer to Arg244 and the *b*3 strand. This proximity to the oxyanion hole, formed by Ser70 NH and Gly237 NH, implies a slight displacement of WAT295 which interacts with Gly237 NH, SUL291 O1 and Ser70 OG, whereas the equivalent water molecule in the other class A β-lactamase structures is in contact with Gly237 NH, Gly237 O and Ser70 OG.

Accessible surface area

The accessible surface area of the amino acids of the TEM1 structure was computed with the *DSSP* program (Kabsch & Sander, 1983). The value for the whole molecule is 11 344 Å² and its repartition along the sequence is quite similar to that of the Bl structure (Knox & Moews, 1991), which has the same fold. The central α-helix *h*2 and the β-sheet are entirely inaccessible to solvent except the *b*2 strand which is exposed; α-helices *h*4 and *h*5 are less buried, and helices *h*1, *h*6, *h*7, *h*8, *h*9 and

Table 7. *Accessible surface area for residues defining the active-site walls and for all charged residues of the TEM1 structure*

Accessible surface area (ASA) is computed with the *DSSP* program (Kabsch & Sander, 1983). The values are compared with those of the corresponding residues in the other three known class A β-lactamase structures: BI, SaG and Sa. ⟨ASA⟩ represents the mean accessibility observed throughout the TEM1 structures for an amino-acid type.

TEM1		BI		SaG		Sa			
AA	ASA (Å²)	AA	ASA (Å²)	AA	ASA (Å²)	AA	ASA (Å²)	AA	⟨ASA⟩ (Å²)
(*a*) Residues of the active site									
S70	6	S70	9	S70	6	S70	13	S	25
K73	0	K73	0	K73	0	K73	0	K	102
S130	10	S130	14	S130	22	S130	25	S	25
D131	0	D131	0	D131	0	D131	0	D	51
N132	14	N132	10	N132	17	N132	12	N	94
E166	1	E166	1	E166	0	E166	5	E	78
N170	13	N170	28	N170	19	N170	14	N	94
K234	0	K234	0	K234	0	K234	2	K	102
S235	0	T235	4	T235	4	S235	10	S	25
G236	1	G236	4	G236	2	G236	4	G	25
A237	31	A237	34	A237	40	Q237	95	A	21
(*b*) Charged residues									
D50	29	D50	30	D50	15	D50	17	D	51
D131	0	D131	0	D131	0	D131	0		
D157	8	D157	7	D157	4	D157	9		
D179	1	D179	0	D179	2	D179	1		
D214	4	N214	10	N214	23	N214	2		
D233	0	D233	0	D233	5	D233	0		
E37	25	E37	26	E37	22	E37	40	E	78
E48	2	A48	0	A48	0	A48	0		
E89	9	E89	124	E89	117	N89	116		
E166	1	E166	1	E166	0	E166	5		
K32	26	D32	78	R32	99	E32	128	K	102
K73	0	K73	0	K73	0	K73	0		
K234	0	K234	0	K234	0	K234	0		
R164	27	R164	58	R164	50	R164	40	R	86
R244	24	R244	25	N244	0	R244	24		
R259	46	V259	8	I259	3	I259	0		
R275	31	D275	88	D275	48	N275	90		

*h*11 present an amphiphilic profile. The other structural elements and loops are exposed to the solvent.

The solvent accessibilities of the amino-acid residues defining the active-site walls are compared for the four class A β-lactamase structures (Table 7*a*). Relative to the mean values observed for each type of amino acid throughout the TEM1 structure, the accessibility of residues S70, K73, S130, N132, E166, N170, K234, S235 and G236, that are directly involved in the dense hydrogen-bonding network of the catalytic cleft, is very low. The side chains of D131 and A237 are outside the active pocket. The first, D131, is entirely buried and interacts with side chains and backbone atoms of the α-domain. It would stabilize the position of the SDN loop relatively to the catalytic cleft (Jacob *et al.*, 1990). The second one, A237, is exposed to the solvent and is more variable among class A β-lactamases than the other active-site residues. It is replaced by Gly, Ser, Thr or Gln. Its backbone atoms, pointing towards the active site, would interact with β-lactam compounds during their hydrolysis (Lamotte-Brasseur *et al.*, 1991).

The mean-accessibility value associated with glycine residues is relatively high compared to those observed for alanine and serine. This is due to the fact that the glycine residues in TEM1 are more often located on solvent-exposed loops.

The accessibility analysis also reveals very low values for some charged residues (Table 7*b*). These buried charged residues are generally very well conserved in the class A β-lactamases. They are either involved in the enzymatic activity and/or in the structure stability On the one hand, K73, E166 and K234 would directly participate in the β-lactam ring hydrolysis. On the other hand, D131, R164 and D179 would have an indirect function in maintaining the active-site geometry, as described below.

Arg244, located near the *b*3 strand, is not a conserved residue in class A β-lactamases, indeed in the SaG structure, it is replaced by an asparagine. However, structure comparisons show that the guanidinium group of R220 in SaG is in a position similar to that of R244 in TEM1 (Fig. 10), and the class A β-lactamase sequence alignment reveals that if there is no arginine in position 244, there is generally one in position 220 (or less often in 276, structurally close to 220). This suggests that both arginines R220 and R244 could have the same function in class A β-lactamases. In fact, site-directed mutagenesis experiments and enzymatic analysis have been carried out on TEM1 (Delaire, Labia, Samama & Masson, 1992; Zafaralla, Manavathu, Lerner & Mobashery, 1992) and on SaG (Jacob-Dubuisson, Lamotte-Brasseur, Dideberg, Joris & Frère, 1991). They

confirm that the positive charge of the arginine plays an important role in positioning the substrate in the active site.

Residues E27, E48, E89, K32 and R259 are directly involved in salt bridges specific to the TEM1 structure, except for the E37–R61 interaction which is relatively well conserved among other class A enzymes, and which links the N-terminal helix to the β-sheet.

The other charged residues, with weak solvent exposure D50, D157 and R275, make internal electrostatic interactions, allowing the stabilization of the (*b*1, *b*2) loop, ensuring a large polypeptide chain curvature (G156-D157), and bending the C-terminal helix to the β-sheet.

The role of Asp214 and Asp233 is more ambiguous and some site-directed mutagenesis experiments would be required to elucidate their possible structural and/or functional implication. They are located just above the KTG motif and are involved in interactions with K234 and S130 *via* the internal water molecule WAT298 relatively well conserved among class A structures. In fact D214 and D233 are hydrogen bonded, suggesting that at least one of them is protonated (Fig. 11*a*). In the other class A structures, Asp214 is replaced by an asparagine, but an aspartate at position 246 is also buried and is involved in the same type of interaction with D233 (Fig. 11*b*). Interestingly, all class A β-lactamase sequences contain D214–I246 or N214–D246 pairs, suggesting a special function for the conserved amino acid D233.

Refined structure of the TEM1 S235A mutant

The crystal structure of the S235A mutant was rapidly determined by the molecular-replacement method and Fourier difference synthesis using the atomic coordinates of the native structure. Initial maps were computed with coefficients $(2F_o - F_c)$ and $(F_o - F_c)$, and the model was modified according to the electron density. After several cycles of simulated annealing and individual *B*-factor refinements, the crystallographic *R*-factor value was 17.6% in the 6–2 Å resolution range, including 13 171 reflections with $I \geq 2\sigma(I)$.

As expected, the final refined mutant structure is very close to the native one, and presents an insignificant r.m.s. value of 0.41 Å between all the atoms of the polypeptide chain. In addition to the absence of the OG235 side chain, the comparison of the mutant and the native TEM1 structures reveals an additional water

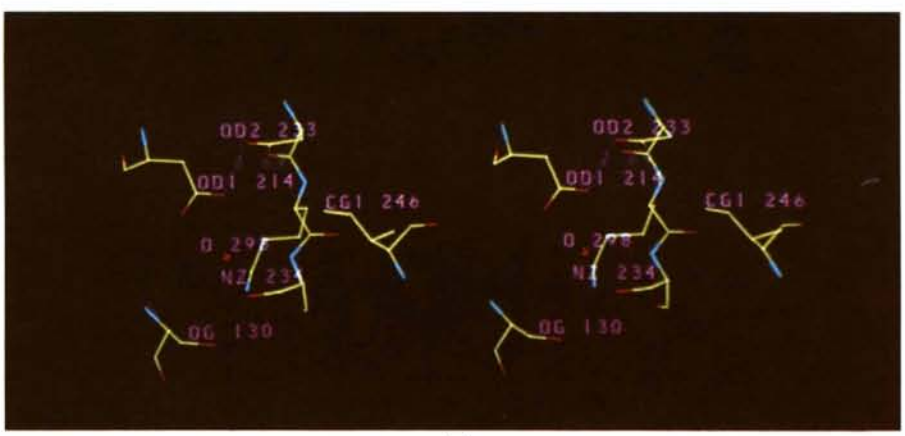

(*a*)

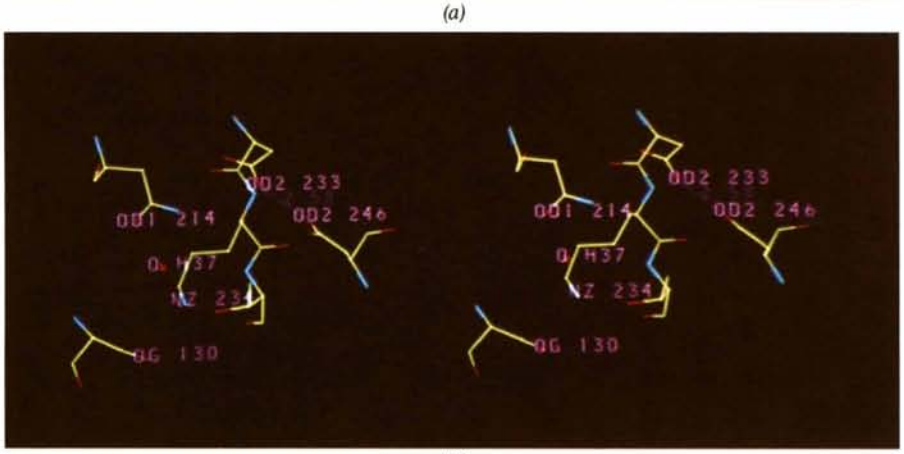

(*b*)

Fig. 11. Two possible interactions of Asp233. (*a*) D214-D233-I246 in TEM1 and (*b*) N214-D233-D246 in SaG.

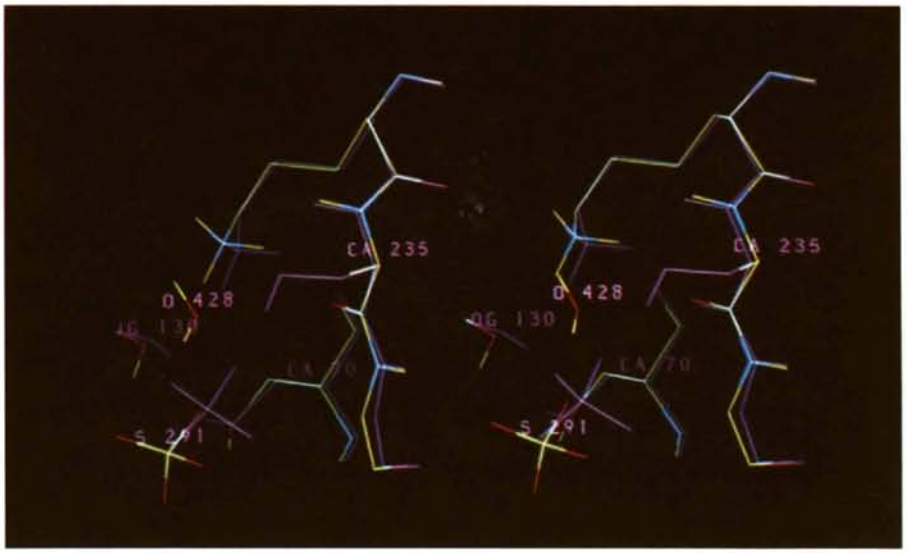

Fig. 12. Superposition of the active sites of TEM1 (magenta) and of its S235A mutant.

molecule, WAT428, near the CB235, which should be incompatible with a bigger side chain at this position (Fig. 12). Indeed, the distance between the O atom of WAT428 and OG235 would be 2.2 Å. This new solvent molecule in the active site introduces some very small perturbations such as the displacement of the sulfate ion and of the other water molecules. Consequently, very slight motions of the side chains 70, 130, 166, pointing into the active site, are also observed (Table 5).

In fact, the hydroxy group of the conserved residue 235, which is either a serine or a threonine in all β-lactamases, appears to be well positioned to interact with the substrate-free carboxylate (Lamotte-Brasseur *et al.*, 1991). Nevertheless, the kinetic parameters obtained for both wild-type and S235A mutant enzymes reveal that the disappearance of this functional group has little impact on the penicillinase activity. On the contrary, the cephalosporinase profile is much more affected (Dubus *et al.*, 1995). The hydroxy group of residue 235 would then be more important for positioning the cephalosporins in the active site of the class A β-lactamases. On the basis of these results, it might be possible to solve the structure of the TEM S235A mutant β-lactamase complexed with a cephalosporin-type substrate.

The atomic coordinates of the TEM1 β-lactamase and of the S235A mutant have been deposited in the Protein Data Bank.*

This work was supported in part by the Belgian programme on Inter-University Poles of Attraction initiated by the Belgian State, Prime Minister's Office, Science Policy Programming (PAI No. 19), an Action Concertée with the Belgian Government (89-94/130), and a Convention tripartite between the Region Wallonne, SmithKline Beecham, UK, and the University of Liège.

* Atomic coordinates have been deposited with the Protein Data Bank, Brookhaven National Laboratory. Free copies may be obtained through The Managing Editor, International Union of Crystallography, 5 Abbey Square, Chester CH1 2HU, England (Reference: GR0390).

References

AMBLER, R. P., COULSON, A. F. W., FRÈRE, J.-M., GHUYSEN, J.-M., JORIS, B., FORSMAN, M., LEVESQUE, R. C., TIRABY, G. & WALEY, S. G. (1991). *Biochem. J.* **276**, 269–272.

AMMAN, E., BROSIUS, J. & PTASHNE, M. (1983). *Gene*, **25**, 168–178.

BERNSTEIN, F. C., KOETZLE, T. F., WILLIAMS, G. J. B., MEYER, E. F., BRICE, M. D., RODGERS, J. R., KENNARD, O., SHIMANOUCHI, T. & TASUMI, M. (1977). *J. Mol. Biol.* **112**, 535–542.

BRANNIGAN, J., SPRATT, B. G., MATAGNE, A., JACOB, F., DAMBLON, C., JORIS, B. & FRÈRE, J.-M. (1991). *Biochem. J.* **278**, 673–678.

BRÜNGER, A. T. (1992). *X-PLOR. A System for Crystallography and NMR, Version* 3.0, *Manual*, Yale Univ., New Haven, CT, USA.

CROWTHER, R. A. (1972). *The Molecular Replacement Method*, edited by M. G. ROSSMANN, pp. 173–185. New York: Gordon and Breach.

CROWTHER, R. A. & BLOW, D. M. (1967). *Acta Cryst.* **23**, 544–548.

DELAIRE, M., LABIA, R., SAMAMA, J.-P. & MASSON, J.-M. (1992). *J. Biol. Chem.* **267**, 20600–20606.

DIDEBERG, O., CHARLIER, P., WERY, J.-P., DEHOTTAY, P., DUSART, J., ERPICUM, T., FRÈRE, J.-M. & GHUYSEN, J.-M. (1987). *Biochem. J.* **245**, 911–913.

DUBUS, A., WILKIN, J.-M., RAQUET, X., NORMARK, S. & FRÈRE, J.-M. (1995). *Biochem. J.* In the press.

ELLERBY, L. M., ESCOBAR, W. A., FINK, A. L., MITCHINSON, C. & WELLS, J. A. (1990). *Biochemistry*, **29**, 5797–5806.

FITZGERALD, P. M. D. (1988). *J. Appl. Cryst.* **21**, 273–278.

GIBSON, R. M., CHRISTENSEN, H. & WALEY, S. G. (1990). *Biochem. J.* **271**, 399–406.

HEALEY, W. J., LABGOLD, M. R. & RICHARDS, J. H. (1989). *Proteins Struct. Funct. Genet.* **6**, 275–283.

HERZBERG, O. (1991). *J. Mol. Biol.* **217**, 701–719.

HERZBERG, O., KAPADIA, G., BLANCO, B., SMITH, T. S. & COULSON, A. (1991). *Biochemistry*, **30**, 9503–9509.

HOWARD, A. J., GILLILAND, G. L., FINZEL, B. C., POULOS, T. L., OHLENDORF, D. H. & SALEMME, F. R. (1987). *J. Appl. Cryst.* **20**, 383–387.

HULETSKY, A., KNOX, J. R. & LEVESQUE, R. C. (1993). *J. Biol. Chem.* **268**, 3690–3697.

JACOB, F., JORIS, B. LEPAGE, S. DUSART, J. & FRÈRE, J.-M. (1990). *Biochem. J.* **271**, 399–406.

JACOB-DUBUISSON, F., LAMOTTE-BRASSEUR, J., DIDEBERG, O., JORIS, B. & FRÈRE, J.-M. (1991). *Protein Eng.* **4**, 811–819.

JACOBY, G. A. & MEDEIROS, A. A. (1991). *Antimicrob. Agents Chemother.* **35**, 1697–1704.

JELSCH, C., MOUREY, L., MASSON, J.-M. & SAMAMA, J.-P. (1993). *Proteins Struct. Funct. Genet.* **16**, 364–383.

JONES, T. A. (1985). *Methods Enzymol.* **115**, 157–171.

JONES, T. A., ZOU, J. Y., COWAN, S. W. & KJELDGAARD, M. (1991). *Acta Cryst.* A**47**, 110–119.

JORIS, B. GHUYSEN, J.-M., DIVE, G., RENARD, A., DIDEBERG, O., CHARLLIER, P., FRÈRE, J.-M., KELLY, J. A., BOYINGTON, J. C., MOEWS, P. C. & KNOX, J. R. (1988). *Biochem. J.* **250**, 313–324.

JORIS, B., LEDENT, P., DIDEBERG, O., FONZÉ, E., LAMOTTE-BRASSEUR, J., KELLY, J. A., GHUYSEN, J.-M. & FRÈRE, J.-M. (1991). *Antimicrob. Agents Chemother.* **35**, 2294–2301.

JUTEAU, J.-M., BILLINGS, E., KNOX, J. R. & LEVESQUE, R. C. (1992). *Protein Eng.* **5**, 693–701.

KABSCH, W. & SANDER, C. (1983). *FEBS Lett.* **155**, 179–182.

KELLY, J. A., DIDEBERG, O., CHARLIER, P., WERY, J.-P., LIBERT, M., MOEWS, P. C., KNOX, J. R., DUEZ, C., FRAIPONT, C., JORIS, B., DUSART, J., FRÈRE, J.-M. & GHUYSEN, J.-M. (1986). *Science*, **231**, 1429–1431.

KNOX, J. R. & MOEWS, P. C. (1991). *J. Mol. Biol.* **220**, 435–455.

KNOX, J. R., MOEWS, P. C., ESCOBAR, W. A. & FINK, A. L. (1993). *Protein Eng.* **6**, 11–18.

LAMOTTE-BRASSEUR, J., DIVE, G., DIDEBERG, O., CHARLIER, P., FRÈRE, J.-M. & GHUYSEN, J.-M. (1991). *Biochem. J.* **279**, 213–221.

LATTMAN, E. E. & LOVE, W. E. (1970). *Acta Cryst.* B**26**, 1854–1857.

LEDENT, P., RAQUET, X., JORIS, B., VAN BEEUMEN, J. & FRÈRE, J.-M. (1993). *Biochem. J.* **292**, 555–562.

LENFANT, F., LABIA, R. & MASSON, J.-M. (1990). *Biochimie*, **72**, 495–503.

LOBKOVSKY, E., MOEWS, P. C., LIU, H., ZHAO, H., FRÈRE, J.-M. & JAMES, R. K. (1993). *Proc. Natl Acad. Sci. USA*, **90**, 11257–11261.

LUZZATI, V. (1952). *Acta Cryst.* **5**, 802–810.

MATAGNE, A. & FRÈRE, J.-M. (1995). *Biochim. Biophys. Acta*. In the press.

MOEWS, P. C., KNOX, J. R., DIDEBERG, O., CHARLIER, P. & FRÈRE, J.-M. (1990). *Proteins Struct. Funct. Genet.* **7**, 156–171.

NAVAZA, J. (1994). *Acta Cryst.* A**50**, 157–163.

NORDMANN, P. & NAAS, T. (1994). *Antimicrob. Agents Chemother.* **38**, 104–114.

OEFNER, C., D'ARCY, A., DALY, J. J., GUBERNATOR, K., CHARNAS, R. L., HEINZE, I., HUBSCHWERFEN, C. & WINKLER, F. K. (1990). *Nature (London)*, **343**, 284–288.

RAMACHANDRAN, G. N., RAMAKRISHNAN, C. & SASISEKHARAN, V. (1963). *J. Mol. Biol.* **7**, 955–999.

SCHULZ, S. C. , DALBADIE-MCFARLAND, G., NEITZEL, J. J. & RICHARDS, J. H. (1987). *Proteins Struct. Funct. Genet.* **2**, 290–297.

SOWEK, J. A., SINGER, S. B., OHRINGER, S., MALLEY, M. F., DOUGHERTY, T. J., GOUGOUTAS, J. Z. & BUSH, K. (1991). *Biochemistry*, **30**, 3179–3188.

STRYNADKA, N. C. J., ADACHI, H., JENSEN, S. E., JOHNS, K., SIELECKI, A., BETZEL, C., SUTOH, K. & JAMES, M. N. G. (1992). *Nature (London)*, **359**, 700–705.

WALEY, S. G. (1992). *The Chemistry of β-Lactams*, edited by M. I. PAGE, pp. 198–225. Glasgow: Blackie.

ZAFARALLA, G., MANAVATHU, E. K., LERNER, S. A. & MOBASHERY, S. (1992). *Biochemistry*, **31**, 3847–3852.